Efficient Transplantation via Antibody-Based Clearance of Hematopoietic Stem Cell Niches

Agnieszka Czechowicz *et al.*

The relaxation at T_g is characterized by a large decrease of the storage modulus (28). The main relaxation in the vicinity of T_g is not seen in the presence of CNTs. The storage modulus is less temperature-dependent and reflects a broadening of the glass transition. It has been shown that large gradients of T_g can develop at the interface of nanoparticles (29). The transition can be shifted up by more than 100°C when the polymer is confined at 1 nm from the interface and by only a few degrees Celsius at 10 nm (29). The effect becomes negligible at greater distances. The average diameter of the polymer layers around the CNTs is $D = r/\sqrt{\phi}$, where r is the average diameter of the CNT bundles, and ϕ is the CNT volume fraction. This yields $D = 11$ nm by assuming $r \sim 5$ nm and an equal density for the CNTs and the polymer (24). The polymer shells around the CNTs largely overlap and percolate, such as the CNTs themselves, meaning that there is a distribution of polymer-to-CNT distances that ranges from molecular contact to several nanometers. This distribution of confinement results in a wide broadening of the relaxation-time spectrum and specifically the glass transition through a distribution of polymer fractions that exhibit different T_g. This property is responsible for peaks of stress recovery well above the T_g of the neat polymer. Indeed, when the material is stretched at T_d, the polymer fractions that have lower T_g (far from the interface) can quickly relax and do not efficiently participate in the storage of mechanical energy. In contrast, polymer fractions with T_g close to T_d dominate the behavior by storing and restoring mechanical energy. Composites treated in the vicinity of T_g of the neat polymer still exhibit higher toughness and generate greater stress recovery than those treated at temperatures well above T_g of the neat polymer. This indicates that the fractions of amorphous polymer with unshifted or slightly shifted T_g remain the major components of the composite. Polymer fractions with strongly shifted glass transition are confined in smaller volumes closer to the interface of the nanotubes. The effect of the polymer fractions with high T_g is thus less pronounced. The lower volume of more confined polymer results in lower recovery stress at high temperatures, as experimentally observed. The decreasing volume of polymer fractions closer to the CNT interfaces can also contribute in sharpening memory effects. Polymer fractions with T_g above T_d can participate in the shape-memory behavior, but their volume becomes smaller as we consider higher T_d. This lowers the recovery stress above T_d and contributes in defining more precisely the temperature of maximal recovery stress.

The phenomena investigated herein, and shape-memory properties in general, are expected to depend on kinetics, such as the glass transition of conventional polymers. But relaxations in glasses become exponentially slow or fast when the temperature is shifted, respectively, below or above temperatures of the glass transition region. The present effects have been observed from 70°

to 180°C in the same conditions, meaning that temperature memorization is not incidentally due to the heating rate. Preliminary experiments with a heating rate of 1°C/min confirmed this feature and yielded the same temperature-memory behavior. Furthermore, the intrinsic mechanical properties of the CNTs are not expected to play a critical role in the investigated phenomena because the levels of mechanical stresses are too low to achieve large deformations of the CNTs. The Young's modulus of CNTs is several hundred gigapascals (30), whereas the maximal stress of the composite fibers during deformation does not exceed 0.5 GPa. However, polymer nanoconfinement and the high fraction of CNTs are essential features to achieve temperature-memory and strong shape-memory effects through alterations of the thermomechanical properties of the polymer.

References and Notes
1. E. Hornbogen, *Adv. Eng. Mater.* **8**, 101 (2006).
2. A. Lendlein, S. Kelch, *Angew. Chem. Int. Ed.* **41**, 2034 (2002).
3. J. Van Humbeeck, *Adv. Eng. Mater.* **3**, 837 (2001).
4. B. K. Kim, S. Y. Lee, M. Xu, *Polymer* **37**, 5781 (1996).
5. T. Ohki, Q.-Q. Ni, N. Ohsako, M. Iwamoto, *Compos. Part A Appl. Sci. Manuf.* **35**, 1065 (2004).
6. J. Hu, Z. Yang, L. Yeung, F. Ji, Y. Liu, *Polym. Int.* **54**, 854 (2005).
7. J. Morshedian, H. A. Khonakdar, M. Mehrabzadeh, H. Eslami, *Adv. Polym. Technol.* **22**, 112 (2003).
8. K. Gall et al., *J. Biomed. Mater. Res. Part A* **73a**, 339 (2005).
9. R. D. Kornbluh et al., *Proc. SPIE* **4698**, 254 (2002).
10. A. Lendlein, R. Langer, *Science* **296**, 1673 (2002); published online 25 April 2002 (10.1126/science.1066102).
11. V. B. Gupta, J. Radhakrishnan, S. K. Sett, *Polymer* **35**, 2560 (1994).
12. E. Patoor, D. C. Lagoudas, P. B. Entchev, L. C. Brinson, X. Gao, *Mech. Mater.* **38**, 391 (2006).
13. D. C. Lagoudas et al., *Mech. Mater.* **38**, 430 (2006).
14. K. Gall, M. L. Dunn, Y. Liu, G. Stefanic, D. Balzar, *Appl. Phys. Lett.* **85**, 290 (2004).
15. Y. Liu, K. Gall, M. L. Dunn, P. McCluskey, *Mech. Mater.* **36**, 929 (2004).
16. K. Gall et al., *Acta Mater.* **50**, 5115 (2002).
17. Q. Meng, J. Hu, Y. Zhu, *J. Appl. Polym. Sci.* **106**, 837 (2007).
18. H. Koerner, G. Price, N. A. Pearce, M. Alexander, R. A. Vaia, *Nat. Mater.* **3**, 115 (2004).
19. R. Mohr et al., *Proc. Natl. Acad. Sci. U.S.A.* **103**, 3540 (2006).
20. G. M. Spinks, V. Mottaghitalab, M. Bahrami-Saniani, P. G. Whitten, G. G. Wallace, *Adv. Mater.* **18**, 637 (2006).
21. S. V. Ahir, E. M. Terentjev, *Nat. Mater.* **4**, 491 (2005).
22. A. B. Dalton et al., *Nature* **423**, 703 (2003).
23. P. Miaudet et al., *Nano Lett.* **5**, 2212 (2005).
24. See supporting materials available on *Science* Online.
25. B. Vigolo et al., *Science* **290**, 1331 (2000).
26. Y. Miyamoto, K. Fukao, H. Yamao, K. Sekimoto, *Phys. Rev. Lett.* **88**, 225504 (2002).
27. M. Cadek et al., *Nano Lett.* **4**, 353 (2004).
28. J.-S. Park, J.-W. Park, E. Ruckenstein, *J. Appl. Polym. Sci.* **82**, 1816 (2001).
29. J. Berriot, H. Montes, F. Lequeux, D. Long, P. Sotta, *Europhys. Lett.* **64**, 50 (2003).
30. B. I. Yakobson, L. S. Couchman, in *Dekker Encyclopedia of Nanoscience and Nanotechnology* (Taylor & Francis Group, New York, 2004), pp. 587–601.
31. We thank J. L. Barrat for fruitful discussions about gradients of T_g in nanocomposites. This work was financially supported by the Délégation Générale pour l'Armement and the Conseil Régional d'Aquitaine.

Efficient Transplantation via Antibody-Based Clearance of Hematopoietic Stem Cell Niches

Agnieszka Czechowicz, Daniel Kraft, Irving L. Weissman,*† Deepta Bhattacharya†

Upon intravenous transplantation, hematopoietic stem cells (HSCs) can home to specialized niches, yet most HSCs fail to engraft unless recipients are subjected to toxic preconditioning. We provide evidence that, aside from immune barriers, donor HSC engraftment is restricted by occupancy of appropriate niches by host HSCs. Administration of ACK2, an antibody that blocks c-kit function, led to the transient removal of >98% of endogenous HSCs in immunodeficient mice. Subsequent transplantation of these mice with donor HSCs led to chimerism levels of up to 90%. Extrapolation of these methods to humans may enable mild but effective conditioning regimens for transplantation.

Allogeneic bone marrow transplantation (BMT) generally requires conditioning of the recipient through cytoreductive treatments to prevent immunological rejection of the graft. Because these regimens can be associated with serious side effects (1), such preparative treatments are often omitted for patients with diseases such as severe combined immuno-

deficiency (SCID), as these patients are incapable of rejecting donor grafts (2). Nonetheless, although large numbers of B and T lymphocytes are at least transiently generated, the levels of donor HSC engraftment are usually less than 1% after transplantation into unconditioned SCID recipients (3–6). Although several studies have concluded that transplanted HSCs can easily replace

endogenous HSCs without conditioning (7, 8), earlier studies suggested that the availability of niches is a limiting factor to transplantation (9). Thus, we reasoned that donor HSC engraftment might be limited by the occupancy of appropriate niches by endogenous HSCs, and that the development of reagents that specifically remove host HSCs could lead to safer transplantation-based therapies for hematological and nonhematological disorders than those currently in use.

To address whether endogenous HSCs could be replaced by transplanted HSCs in a linear dose-dependent manner, we transplanted unconditioned Rag2$^{-/-}$ γc$^{-/-}$ mice (10, 11) with varying numbers of c-kit$^+$ lineage$^-$ Sca-1$^+$ (KLS) CD34$^-$ CD150$^+$ HSCs from mice expressing green fluorescent protein (GFP) driven by the β-actin promoter (12–16). Peripheral blood granulocyte chimerism was measured at 16 weeks after transplant; this method has been shown to accurately reflect donor HSC chimerism in this system (3, 15). Donor granulocyte chimerism increased measurably in doses of 10 to 250 transplanted HSCs, but transplantation of more than 250 cells led to at most modest increases in chimerism (Fig. 1). Transplantation of 18,000 HSCs, representing ~70% of the total number of HSCs in an adult mouse (17, 18), led to a mean chimerism of only 3% (Fig. 1, top panel). Similar results were obtained through transplantation of unfractionated bone marrow (12) (fig. S1). These data suggest that without conditioning, HSC engraftment is limited by the number of saturable niches that are empty at the time of transplant or become empty as the transplanted cells still survive.

To determine the specificity of these niches, we competitively transplanted unconditioned Rag2$^{-/-}$ γc$^{-/-}$ (CD45.2) mice with 1000 CD45.1 HSCs along with 100,000 GFP$^+$ KLS CD34$^+$ progenitor cells, which are the immediate progeny of HSCs (16, 19). No significant difference in donor HSC chimerism was observed in these mice relative to recipients that received 1000 HSCs alone ($P = 0.77$) (Fig. 1, lower right panel), which suggests that HSCs and their immediate progeny use distinct niches to maintain function.

To determine whether the specific elimination of host HSCs would allow for high levels of donor HSC engraftment, we compared a number of different candidate HSC-depleting monoclonal antibodies, including α-Sca1 (13), α-integrin α4 (20), and α-ESAM1 (21), but ultimately selected ACK2, an antibody known to recognize and antagonize c-kit (22), the receptor for stem cell factor (SCF) (23). We reasoned that if the ACK2 antibody were capable of depleting endogenous HSCs, residual antibody in the serum of mice would also deplete transplanted donor HSCs. To determine the

kinetics of antibody clearance in vivo, we administered ACK2 intravenously to Rag2$^{-/-}$ γc$^{-/-}$ mice and tested the serum for the presence of antibody (12). ACK2 remained in the serum until 5 days after injection; however, no ACK2 was detected by 7 or 8 days after injection (Fig. 2A). All mice survived the ACK2 treatment with no obvious signs of distress (12) (table S1 and fig. S2). At this

time point, a ~99% decrease in the number of HSCs (Fig. 2B) was observed, and comparable levels of depletion were observed in B cell–deficient and wild-type mice (12) (fig. S3). To further confirm HSC depletion, we transplanted 200,000 bone marrow cells into lethally irradiated recipients 9 days after ACK2 treatment (12). Transplantation of bone marrow from ACK2-

Fig. 1. Available HSC niches can be saturated with donor HSCs. Peripheral blood of transplanted unconditioned RAG2$^{-/-}$ γc$^{-/-}$ mice was analyzed 16 weeks after HSC transplantation for GFP$^+$ granulocytes. The lower panel represents an expanded view of results from transplantation of 10 to 1000 HSCs. In the lower right panel, mice were cotransplanted with 1000 CD45.1 HSCs and 100,000 GFP$^+$ KLS CD34$^+$ cells. Mean values ± SEM are shown ($n = 4$ or 5 for each dose); **$P < 0.05$ relative to the chimerism arising from the 10 HSC–transplanted group. The dashed line represents the theoretical HSC chimerism if engraftment were to increase linearly with transplanted cell dose from the observed chimerism at the 50 HSC–dose group.
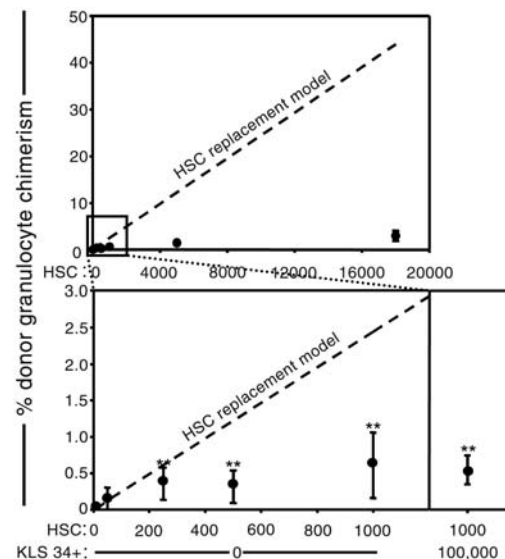

Fig. 2. ACK2 treatment depletes HSCs in vivo. (**A**) ACK2 is cleared from serum of RAG2$^{-/-}$ γc$^{-/-}$ mice 7 days after injection. Serum of mice receiving 500 μg of ACK2 was analyzed every 2 days for ACK2 antibody by staining c-kit$^+$ mast cells (31). (**B**) ACK2 administration leads to depletion of bone marrow HSCs. Numbers of KLS CD135$^-$ CD150$^+$ HSCs were determined in femurs and tibia of ACK2-treated and control mice. Mean values ± SEM are shown ($n = 3$ for each time point); **$P < 0.001$. (**C**) ACK2 treatment, but not 2B8 treatment, depletes functional HSCs from bone marrow. We transplanted 200,000 unfractionated bone marrow cells from RAG2$^{-/-}$ γc$^{-/-}$ mice, treated with 500 μg of ACK2 or 2B8 9 days earlier, into wild-type irradiated recipients alongside 200,000 untreated competitor wild-type bone marrow cells. Mean values ± SEM are shown ($n = 5$ to 8); **$P < 0.01$. (**D**) ACK2 treatment does not directly cause HSC mobilization
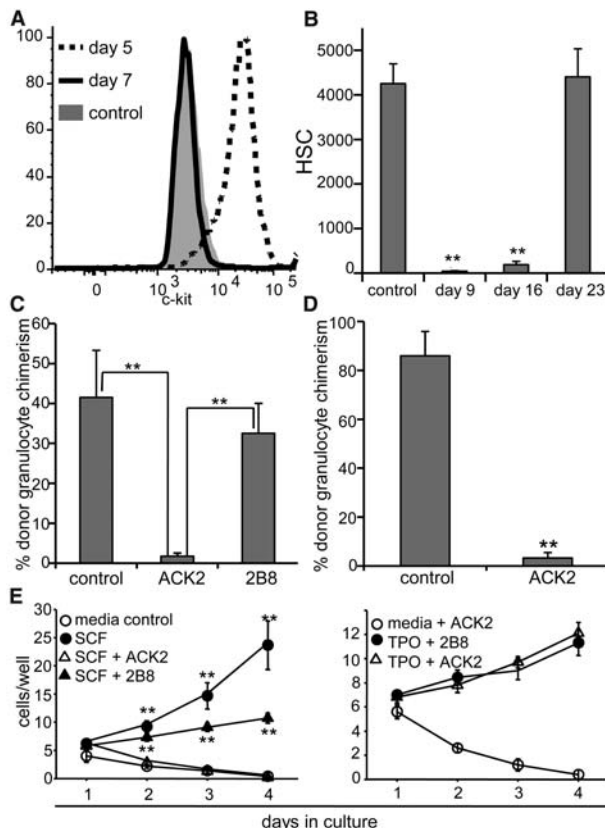
to the spleen. Entire splenocyte populations from mice treated with 500 μg of ACK2 9 days earlier were transplanted alongside 200,000 competitor bone marrow cells from wild-type mice. Mean values ± SEM are shown ($n = 3$ to 9); **$P < 0.001$. (**E**) ACK2 inhibits SCF-mediated HSC proliferation. HSCs were isolated from wild-type mice, plated at 10 cells per well cultured in the presence of SCF or TPO and ACK2 or 2B8. Proliferation was observed by light microscopy. **$P < 0.05$ as compared to ACK2-treated samples.

Institute of Stem Cell Biology and Regenerative Medicine, Departments of Pathology and Developmental Biology, Stanford University School of Medicine, Stanford, CA 94305, USA.

*To whom correspondence should be addressed. E-mail: irv@stanford.edu
†These authors contributed equally to this work.

treated animals led to >90% lower engraftment relative to controls (Fig. 2C), thus confirming that ACK2 depletes functional HSCs from the bone marrow.

To determine the mobilizing effects of ACK2 treatment, we transplanted the entire splenocyte populations of ACK2-conditioned animals into lethally irradiated recipients (12). The donor chimerism resulting from ACK2-treated splenocytes was reduced by >95% relative to controls (Fig. 2D). These data indicate that ACK2 treatment does not induce HSC depletion from the bone marrow by mobilizing HSCs to the spleen. Moreover, we were unable to detect HSCs in the spleen, liver, or blood after ACK2 treatment by flow cytometry (fig. S4). Mobilization was only observed during the recovery phase, well after ACK2 had already cleared from the serum (fig. S5).

To determine the mechanism by which ACK2 depletes HSCs, we compared the effects of ACK2 treatment to that of 2B8, another c-kit monoclonal antibody of the same IgG2b isotype. 2B8 treatment did not decrease functional HSC numbers in vivo, as transplantation of bone marrow cells from mice treated with 2B8 resulted in levels of engraftment similar to those of controls (Fig. 2C). Next, we cultured purified HSCs in the presence of ACK2 and found that it completely inhibited SCF-dependent proliferation, but not thrombopoietin (TPO)–mediated proliferation (Fig. 2E) (12). These data, along with data showing that distinct c-kit–expressing progenitors are depleted at differential rates (12) (fig. S6), suggest that ACK2 does not deplete through Fc-mediated functions. Rather, consistent with studies using c-kit mutant mice (12, 24, 25), the complete inhibition of c-kit signaling by ACK2 (Fig. 2E) can deplete HSCs, whereas the partial inhibition by 2B8 cannot.

By 23 days after treatment, HSC cell surface profiles (fig. S5) and numbers (Fig. 2B) had returned to near normal levels. These data indicate that ACK2 causes a marked but transient depletion of host HSCs and results in a short window during which ACK2-treated animals might be receptive to donor HSC transplantation. To test whether the ablation of host HSCs could improve the efficiency of donor HSC engraftment, we conditioned RAG2$^{-/-}$ (CD45.1) mice with ACK2 and transplanted them with 5000 wild-type CD45.2 HSCs after serum clearance of ACK2. The mean donor granulocyte chimerism at 37 weeks after transplant was 16.1%, reflecting a factor of >10 increase over control recipients (Fig. 3A). These engrafted HSCs also gave rise to peripheral B and T cells (Fig. 3B).

We also analyzed bone marrow HSC chimerism directly at this late time point to confirm the increase in engraftment, and found that it correlated well with peripheral blood granulocyte chimerism (Fig. 3C). Secondary transplants of donor HSCs re-isolated from primary recipients led to multilineage engraftment for at least 16 weeks after transplant (Fig. 3D), confirming that transplanted HSCs regain their normal cell surface phenotype and cell cycle status (fig. S7) by at least 7 to 9 months after transplant in ACK2-treated animals (12).

These data did not distinguish whether ACK2 treatment increased niche space or whether, as in unconditioned animals, only a small fraction of transplanted HSCs initially engrafted but then competitively expanded. If niche space had truly been freed, HSC chimerism would be expected to increase linearly with transplanted cell dose. To distinguish between these alternatives, we transplanted ACK2-conditioned RAG2$^{-/-}$ γc$^{-/-}$ (CD45.2) recipient mice with varying doses of CD45.1 HSCs. Donor engraftment increased linearly with transplanted HSC dose in two independent experiments at both early and late time points (Fig. 4A),
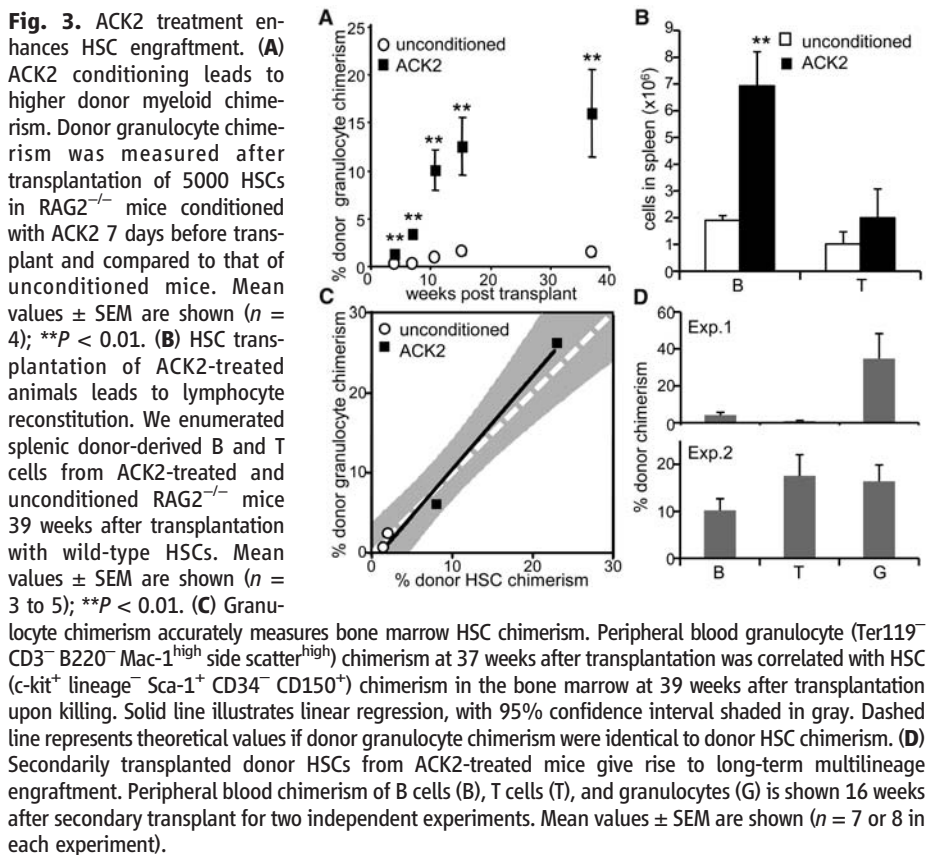
Fig. 3. ACK2 treatment enhances HSC engraftment. (**A**) ACK2 conditioning leads to higher donor myeloid chimerism. Donor granulocyte chimerism was measured after transplantation of 5000 HSCs in RAG2$^{-/-}$ mice conditioned with ACK2 7 days before transplant and compared to that of unconditioned mice. Mean values ± SEM are shown (n = 4); **P < 0.01. (**B**) HSC transplantation of ACK2-treated animals leads to lymphocyte reconstitution. We enumerated splenic donor-derived B and T cells from ACK2-treated and unconditioned RAG2$^{-/-}$ mice 39 weeks after transplantation with wild-type HSCs. Mean values ± SEM are shown (n = 3 to 5); **P < 0.01. (**C**) Granulocyte chimerism accurately measures bone marrow HSC chimerism. Peripheral blood granulocyte (Ter119$^-$ CD3$^-$ B220$^-$ Mac-1^{high} side scatter^{high}) chimerism at 37 weeks after transplantation was correlated with HSC (c-kit$^+$ lineage$^-$ Sca-1$^+$ CD34$^-$ CD150$^+$) chimerism in the bone marrow at 39 weeks after transplantation upon killing. Solid line illustrates linear regression, with 95% confidence interval shaded in gray. Dashed line represents theoretical values if donor granulocyte chimerism were identical to donor HSC chimerism. (**D**) Secondarily transplanted donor HSCs from ACK2-treated mice give rise to long-term multilineage engraftment. Peripheral blood chimerism of B cells (B), T cells (T), and granulocytes (G) is shown 16 weeks after secondary transplant for two independent experiments. Mean values ± SEM are shown (n = 7 or 8 in each experiment).
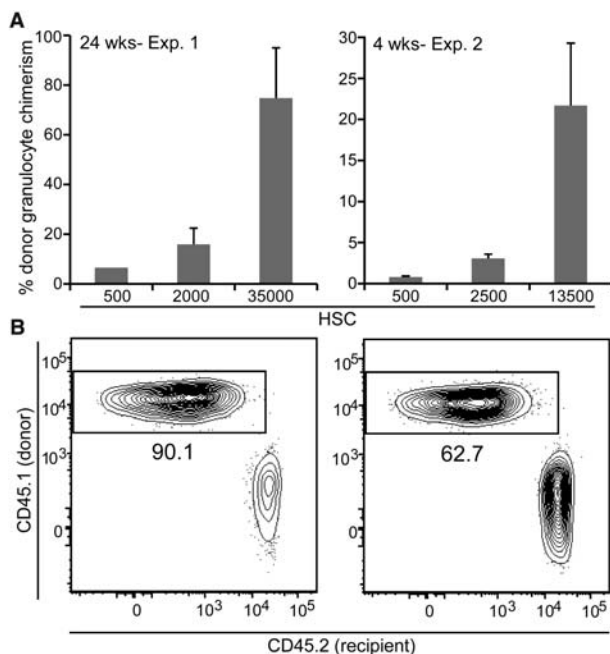

Fig. 4. Donor chimerism increases with transplanted HSC cell number in ACK2-treated mice. (**A**) ACK2 treatment increases available HSC niche space. In two separate experiments, RAG2$^{-/-}$ γc$^{-/-}$ mice were treated with ACK2 and transplanted 9 days later with varying doses of HSCs (CD45.1). Donor granulocyte chimerism was measured as above 24 weeks after transplantation for the first experiment, and 4 weeks after transplantation for the second experiment. Mean values ± SEM are shown. (**B**) Flow cytometry profiles of mice transplanted with 35,000 HSCs. Chimerism of CD3$^-$ B220$^-$ Mac1^{high} side scatter^{high} peripheral blood granulocytes is shown. Numerical values represent percent donor chimerism.

consistent with the emptying of HSC niches by ACK2 treatment. Strikingly, donor chimerism values of up to 90% were achieved at the 35,000 HSC dose (Fig. 4B) and upon repetitive rounds of ACK2 treatment and transplantation of a total of 15,000 HSCs (fig.S8), which, upon extrapolation to humans, is a clinically obtainable number (*12*).

Allogeneic BMT is used routinely for a number of clinical purposes, such as for the treatment of SCID (*26*, *27*). Our results provide evidence that in the absence of conditioning, donor HSC engraftment is limited by the occupancy of appropriate niches by host HSCs. These data offer an explanation for the poor donor HSC engraftment observed in unconditioned SCID patients (*4*, *5*), which in turn may be responsible for the low levels of donor B lymphopoiesis and the finite duration of T cell production (*6*, *28*).

We have shown that administration of ACK2 in vivo leads to the rapid but transient depletion of host HSCs, and that subsequent transplantation of highly purified HSCs leads to donor chimerism levels of up to 90%. When coupled with highly specific immunosuppressive depleting antibodies, shown to be effective in both mice (*29*) and humans (*30*) as transplantation conditioners, the use of HSC-specific depleting antibodies may be an attractive alternative to conventional methods of conditioning [which carry serious health risks (*1*)] and may thus increase the utility of allogeneic BMT for both hematological and nonhematological disorders.

References and Notes

1. C. Ferry, G. Socie, *Exp. Hematol.* **31**, 1182 (2003).
2. R. H. Buckley et al., *J. Med.* **340**, 508 (1999).
3. D. Bhattacharya, D. J. Rossi, D. Bryder, I. L. Weissman, *J. Exp. Med.* **203**, 73 (2006).
4. G. E. Tjonnfjord, R. Steen, O. P. Veiby, W. Friedrich, T. Egeland, *Blood* **84**, 3584 (1994).
5. S. M. Muller, T. Kohn, A. S. Schulz, K. M. Debatin, W. Friedrich, *Blood* **96**, 4344 (2000).
6. M. Cavazzana-Calvo et al., *Blood* **109**, 4575 (2007).
7. G. Brecher, J. D. Ansell, H. S. Micklem, J. H. Tjio, E. P. Cronkite, *Proc. Natl. Acad. Sci. U.S.A.* **79**, 5085 (1982).
8. F. M. Stewart, R. B. Crittenden, P. A. Lowry, S. Pearson-White, P. J. Quesenberry, *Blood* **81**, 2566 (1993).
9. H. S. Micklem, C. M. Clarke, E. P. Evans, C. E. Ford, *Transplantation* **6**, 299 (1968).
10. Y. Shinkai et al., *Cell* **68**, 855 (1992).
11. J. P. Goldman et al., *Br. J. Haematol.* **103**, 335 (1998).
12. See supporting material on *Science* Online.
13. G. J. Spangrude, S. Heimfeld, I. L. Weissman, *Science* **241**, 58 (1988).
14. M. J. Kiel, O. H. Yilmaz, T. Iwashita, C. Terhorst, S. J. Morrison, *Cell* **121**, 1109 (2005).
15. D. E. Wright, A. J. Wagers, A. P. Gulati, F. L. Johnson, I. L. Weissman, *Science* **294**, 1933 (2001).
16. M. Osawa, K. Hanada, H. Hamada, H. Nakauchi, *Science* **273**, 242 (1996).
17. G. A. Colvin et al., *Leukemia* **18**, 575 (2004).
18. K. Sudo, H. Ema, Y. Morita, H. Nakauchi, *J. Exp. Med.* **192**, 1273 (2000).
19. D. J. Rossi et al., *Proc. Natl. Acad. Sci. U.S.A.* **102**, 9194 (2005).
20. D. A. Williams, M. Rios, C. Stephens, V. P. Patel, *Nature* **352**, 438 (1991).
21. E. C. Forsberg et al., *PLoS Genet.* **1**, e28 (2005).
22. M. Ogawa et al., *J. Exp. Med.* **174**, 63 (1991).
23. O. N. Witte, *Cell* **63**, 5 (1990).
24. R. A. Fleischman, B. Mintz, *Proc. Natl. Acad. Sci. U.S.A.* **76**, 5736 (1979).
25. C. L. Miller et al., *Exp. Hematol.* **24**, 185 (1996).
26. F. H. Bach, R. J. Albertini, P. Joo, J. L. Anderson, M. M. Bortin, *Lancet* **ii**, 1364 (1968).
27. R. A. Gatti, H. J. Meuwissen, H. D. Allen, R. Hong, R. A. Good, *Lancet* **ii**, 1366 (1968).
28. M. Sarzotti et al., *J. Immunol.* **170**, 2711 (2003).
29. P. Gambel, L. H. Francescutti, T. G. Wegmann, *Transplantation* **38**, 152 (1984).
30. A. B. Cosimi et al., *J. Med.* **305**, 308 (1981).
31. T. Nakano et al., *J. Exp. Med.* **162**, 1025 (1985).
32. We thank D. Bryder for helpful discussions and technical assistance; L. Jerabek for laboratory management; C. Richter for antibody production; L. Hidalgo, D. Escoto, and J. Dollaga for animal care; C. Park for histological expertise; and M. Longaker and D. Rossi for critical reading of the manuscript. Supported by NIH grants 5R01HL058770 and 5R01CA086065 (I.L.W.), a fellowship from the Medical Scholars Program at Stanford University School of Medicine (A.C.), a fellowship from the Cancer Research Institute and NIH grants T32AI0729022 and 5K01DK078318 (D.B.), and Hope Street Kids Award and NIH grant 5K08HL076335 (D.K.). I.L.W. owns Amgen stock, cofounded and consulted for Systemix, is a cofounder and director of Stem Cells Inc., and cofounded and is a director of Cellerant Inc.

Requirement of Inositol Pyrophosphates for Full Exocytotic Capacity in Pancreatic β Cells

Christopher Illies,[1] Jesper Gromada,[2] Roberta Fiume,[1] Barbara Leibiger,[1] Jia Yu,[1] Kirstine Juhl,[3] Shao-Nian Yang,[1] Deb K. Barma,[4] John R. Falck,[4] Adolfo Saiardi,[5] Christopher J. Barker,[1]* Per-Olof Berggren[1]

Inositol pyrophosphates are recognized components of cellular processes that regulate vesicle trafficking, telomere length, and apoptosis. We observed that pancreatic β cells maintain high basal concentrations of the pyrophosphate diphosphoinositol pentakisphosphate (InsP_7 or IP$_7$). Inositol hexakisphosphate kinases (IP6Ks) that can generate IP$_7$ were overexpressed. This overexpression stimulated exocytosis of insulin-containing granules from the readily releasable pool. Exogenously applied IP$_7$ dose-dependently enhanced exocytosis at physiological concentrations. We determined that IP6K1 and IP6K2 were present in β cells. RNA silencing of IP6K1, but not IP6K2, inhibited exocytosis, which suggests that IP6K1 is the critical endogenous kinase. Maintenance of high concentrations of IP$_7$ in the pancreatic β cell may enhance the immediate exocytotic capacity and consequently allow rapid adjustment of insulin secretion in response to increased demand.

Phosphoinositides have a prominent role in cellular signal-transduction events (*1–3*). Highly phosphorylated inositol polyphosphates, distant derivatives of the inositol 1,4,5-trisphosphate (IP$_3$) second messenger, function in signal-transduction and cellular regulation (*4–6*). The pyrophosphate derivatives of IP$_6$ di-phosphoinositol pentakisphosphate, and bis-(diphospho)inositol tetrakisphosphate are commonly referred to as IP$_7$ and IP$_8$ (also, InsP_7 and InsP_8, respectively). These inositol pyrophosphate derivatives rapidly turnover and are estimated to have similar free energy of hydrolysis to that of adenosine 5′-triphosphate (ATP) (*4*). A strik-ing consequence of this high-energy phosphate group is the ability of IP$_7$ to phosphorylate a subset of proteins directly in an ATP- and enzyme-independent manner (*7*). The variety of cellular responses that are apparently controlled by inositol pyrophosphates (*4*, *8*) may be facilitated by the differential intracellular distribution of the kinases that make them (*9*). The concentrations of inositol pyrophosphates can be dynamically regulated during key cellular events. For example, IP$_7$ concentrations change during cell cycle progression (*10*), and IP$_7$ regulates cyclin–cyclin-dependent kinase complexes (*11*), whereas IP$_8$ increases acutely in response to cellular stress (*8*). IP$_6$ also functions as an enzymatic cofactor (*4*), and so, by analogy, it is possible that even at concentrations found in unstimulated cells, IP$_7$ could be an important regulatory molecule.

[1]The Rolf Luft Research Center for Diabetes and Endocrinology, Karolinska Institutet, SE-171 76, Stockholm, Sweden. [2]Diabetes and Metabolism Disease Area, Novartis Institutes for BioMedical Research, Cambridge, MA 02139, USA. [3]Joslin Diabetes Center, Harvard Medical School, Boston, MA 02215, USA. [4]Department of Biochemistry, University of Texas Southwestern Medical Center, Dallas, TX 75390, USA. [5]U.K. Medical Research Council (MRC) Cell Biology Unit and Laboratory for Molecular Cell Biology, Department of Biochemistry and Molecular Biology, University College London, Gower Street, London WC1E 6BT, UK.

*To whom correspondence should be addressed. E-mail: chris.barker@ki.se